THE JOURNAL OF BIOLOGICAL CHEMISTRY
Vol. 280, No. 31, Issue of August 5, pp. 28388–28393, 2005
Printed in U.S.A.

The Hydrophobic Hinge Region of Rat DNA Polymerase β Is Critical for Substrate Binding Pocket Geometry*

Received for publication, February 25, 2005, and in revised form, April 27, 2005
Published, JBC Papers in Press, May 17, 2005, DOI 10.1074/jbc.M502178200

Daniela Starcevic‡§, Shibani Dalal‡, Joachim Jaeger¶, and Joann B. Sweasy‡‖‡‡**

*From the Departments of ‖Genetics, **Therapeutic Radiology and ‡Program in Microbiology, Yale University School of Medicine, New Haven, Connecticut 06520 and the ¶Center for Medical Sciences, Wadsworth Center, Albany, New York 12201*

The hydrophobic hinge of DNA polymerase β facilitates closing and stabilization of the enzyme once the nucleotide substrate has bound. Alteration of the hydrophobic nature of the hinge by the introduction of a hydrophilic glutamine residue in place of isoleucine 260 results in an inaccurate polymerase. The kinetic basis of infidelity is lack of discrimination during the binding of substrate. The I260Q polymerase β variant has lower affinity than wild type enzyme for the correct substrate and much higher affinity for the incorrect substrate. Our results demonstrate that the hinge is important for formation of the substrate binding pocket. Our results are also consistent with the interpretation that DNA polymerase β discriminates the correct from incorrect substrate during the binding step.

DNA damage poses a daily threat to the survival of eukaryotic cells. This damage, when left unrepaired, can result in mutations, some of which lead to cancer. Among the repair processes that eukaryotic cells have evolved to ensure prompt repair of DNA damage, base excision repair is the pathway responsible for removal of 10,000 lesions per cell per day that result from oxidative and alkylation damage (1–4).

Like other repair processes, base excision repair consists of a sequence of finely tuned events that starts with a specific glycosylase recognizing the damaged base (5). Upon removal of the base by the glycosylase, an apurinic/apyrimidinic exonuclease excises the sugar-phosphate backbone and leaves a gap in the DNA (6, 7). This gap is filled by DNA polymerase β (Polβ)[1] in most base excision repair events. In short patch base excision repair, where only a single base is filled in, Polβ is able to remove the 5′-deoxyribose phosphate with its 5′-deoxyribose phosphate lyase activity (8) thus leaving a substrate ready for completion of repair by a DNA ligase (9).

Polβ has been associated with a variety of other cellular processes including meiosis where it was found to localize to synaptonemal complexes (10, 11). Polβ is necessary for development as evidenced by the fact that a homozygous deletion in mice is lethal (12).

Although Polβ is considered a fairly low fidelity polymerase (13), it performs nucleotide insertion in a template-directed manner where it is able to discriminate and select the correct dNTP from a pool of very similar nucleotide substrates. The inherently lower fidelity of this enzyme can be further attributed to the fact that it does not have any intrinsic proofreading or nuclease activities. However, the lack of these functions makes it ideal for a direct study of incorporation fidelity. Additionally, several crystal structures of DNA polymerase β are available including that of the enzyme bound to the DNA substrate alone, termed the "open" conformation, and that of the enzyme in complex with both the DNA and dNTP substrates, known as the "closed" conformation (14–17). The availability of these structures further aids us in understanding fidelity and allows us to relate the functional and structural information. Polβ is a relatively small enzyme that is easy to purify. Cumulatively, these features make Polβ the ideal candidate for study of enzyme activity and fidelity.

Recently, a variety of Polβ mutants have been found associated with numerous types of human cancers. Of the 149 tumor samples examined, 30% contained mutations in DNA polymerase β (18). Given the known role of polymerase β in DNA repair and the possible role in meiosis as well as its implicated roles in small-scale replicative synthesis, it is of crucial importance to understand the types and nature of mutations that could lead to infidelity. This infidelity can result in the accumulation of mutations that could, in turn, result in cancer and/or abnormalities in cellular processes.

Here we present the biochemical characterization of the I260Q variant of Polβ. Residue Ile-260 is located in the hinge region of DNA polymerase β, which is the region that underlies the area between the fingers and the palm domains of the enzyme (16). Ile-260 appears to be of particular significance for its position at the bottom of the hinge, directly underneath the plane where the DNA substrate is positioned. We previously conducted a genetic screen that identified I260Q as a high activity mutant with low fidelity (19). I260Q was shown to have activity levels comparable with wild type in the *recA718polA12* heterologous complementation system (20). Because wild type Polβ was shown to substitute for Pol I of *Escherichia coli* in the joining of Okazaki fragments, this complementation system assesses the catalytic activity of Polβ mutants that are expressed in the *recA718polA12* strain. Furthermore, in the same system, I260Q reverted the *trpE56* mutation at a frequency 60-fold higher than wild type indicating that this mutant has a strong *in vivo* mutator phenotype (21). We confirmed these findings *in vitro* and found I260Q to have wild type activity levels in a primer extension assay. We also used the *in vitro* primer extension assay to show that the mutator activity is an intrinsic characteristic of I260Q (19).

In the study reported here, we examined the kinetic and

* This work was supported in part by National Institutes of Health NCI Grant CA80830 (to J. B. S.). The costs of publication of this article were defrayed in part by the payment of page charges. This article must therefore be hereby marked "*advertisement*" in accordance with 18 U.S.C. Section 1734 solely to indicate this fact.

§ Partially supported by the Yale and Bristol-Myers Squibb Research Educational Alliance grant.

‡‡ Donaghue Investigator. To whom correspondence should be addressed: Dept. of Therapeutic Radiology and Genetics, Yale University School of Medicine, 333 Cedar St., New Haven, CT 06520. Tel.: 203-737-2626; Fax: 203-785-6309; E-mail: joann.sweasy@yale.edu.

[1] The abbreviation used is: Polβ, polymerase β.

TABLE I
DNA substrates employed in kinetic experiments

The templating base is underlined.

Substrate	Sequence
1B-A	5′-TTGCGACTTATCAACGCCCACACAGTAGCTGTCTTCTCAGTTTC-3′ 3′-AACGCTGAATAGTTGCGGGTGTAGTCATCGACAGAAGAGTCAAAG-5′
1B-C	5′-TTGCGACTTATCAACGCCCACACAGTAGCTGTCTTCTCAGTTTC-3′ 3′-AACGCTGAATAGTTGCGGGTGTCGTCATCGACAGAAGAGTCAAAG-5′

structural basis for the mutator phenotype of the I260Q variant and found that I260Q is able to form all three sets of mispairs opposite both a purine and a pyrimidine. Moreover, the kinetic basis for misincorporations performed by this mutant is in the binding affinity for the dNTP substrate where I260Q has a lower affinity for the correct dNTP and higher affinity for the incorrect dNTP as compared with wild type. Our results suggest that the hinge of Polβ is important for discrimination during the binding of nucleotide substrate.

EXPERIMENTAL PROCEDURES

Bacterial Strains—The strain BL21 DE3 with the genotype F^- *ompT hsdSB*($r_b^-m_b$) *gal dcm* (DE3) was used for protein expression. The wild type enzyme as well as the I260Q variant were expressed from a pET28a vector as previously described (22, 23).

Chemicals and Reagents—Ultrapure deoxynucleoside triphosphates, ATP, and [γ-^{32}P]ATP were purchased from New England Biolabs, Sigma, and Amersham Biosciences, respectively. Oligonucleotides were synthesized by the Keck Molecular Biology Center at Yale University and purified by PAGE.

Purification of Polβ Wild Type and the I260Q Variant—The I260Q mutant was generated by site-directed mutagenesis from the wild type construct in the pET28a vector (Novagen) as previously described (19) to generate an amino-terminal His_6 tag. The proteins were expressed and purified as previously described (22) using a fast liquid chromatography system (AKTA FPLC; Amersham Biosciences) to perform an affinity purification step followed by ion-exchange purification. Based on a Coomassie Blue-stained SDS-PAGE gel, these proteins were >90% homogeneous (data not shown). Protein concentrations were calculated based on ϵ_{280} = 21,200 M^{-1} cm^{-1} and a molecular mass of 40 kDa.

DNA Substrate Preparation for Kinetic Studies—The single base pair-gapped DNA substrates with a 5′-phosphate on the downstream oligonucleotide were used for the misincorporation studies. The sequences of the substrates are shown in Table I. The primer oligonucleotide was labeled at the 5′ end using T4 polynucleotide kinase (New England Biolabs) and [γ-^{32}P]ATP. The rest of the oligonucleotides were phosphorylated at the 5′ end with non-radioactive ATP. Labeled and phosphorylated oligonucleotides were purified through a Microspin P-6 or P-30 column (Bio-Rad) and annealed at a primer:template:downstream oligonucleotide ratio of 1:1.3:1.5 in 50 mM Tris, pH 8.0, 250 mM NaCl. The mixture was incubated at 95 °C for 5 min, slow cooled to 50 °C for 30 min, incubated at 50 °C for 20 min, and then immediately transferred to ice. An 18% polyacrylamide gel followed by autoradiography was used to confirm >90% annealing.

Presteady-state Analyses—Burst reactions were performed in 50 mM Tris-HCl, pH 8.0, 2 mM dithiothreitol, 20 mM NaCl, and 10% glycerol with 300 nM DNA substrate 1B-A and 100 nM enzyme. This buffer was also used for all the other kinetic experiments described in this work. All concentrations given are final concentrations upon mixing. These burst experiments were performed at saturating dNTP concentrations. Reactions were initiated by rapid mixing of the Polβ/DNA and Mg/dNTP solutions. The Rapid Quench apparatus (KinTek) (24) was employed in these experiments because of the fast reaction rate. The reactions were quenched with 0.3 M EDTA.

Active Site Titration—A fixed concentration of either wild type Polβ or the I260Q variant was preincubated with a range of concentrations of the 1B-A substrate followed by reacting with the correct dNTP substrate, dTTP, for 0.3 s. This time interval was chosen based on the burst reaction and ensures maximum reaction amplitude while minimizing multiple turnovers. The results of these reactions were used to calculate the percentage of active sites of the enzyme and the equilibrium dissociation constant for the DNA substrate, K_D, as described below.

Single Turnover Misincorporation Assays—This experimental approach provides a way to compare the I260Q variant with the wild type enzyme for their relative abilities to incorporate correct and incorrect dNTPs into a primer-template by determining the dissociation constant from the dNTP substrate, K_d, and the maximum rate of polymerization for each dNTP, k_{pol}. Single turnover kinetic experiments were performed under conditions in which over 90% of the DNA is bound by the enzyme to ensure that the rate of a single catalytic turnover is being measured. These conditions were empirically determined to be at a 15:1 molar ratio of enzyme to DNA for the I260Q variant (data not shown); therefore, 750 nM enzyme (for both I260Q and wild type) and 50 nM DNA were used with varying concentrations of dNTP. The reactions for correct dNTP incorporation were performed in the KinTek apparatus at 37 °C by loading 15 μl of the Polβ-DNA complex in one sample loop and 15 μl of a single dNTP into the other. Substrate concentrations typically used were 1–100 μM and reactions times were 0–8 s. Misincorporation reactions were performed under the same conditions as for correct dNTP incorporation but manually, with a range of dNTP concentrations between 1 and 1 mM, and reaction times 0–2700 s.

Product Separation and Data Analysis—All the reactions described above resulted in the addition of one nucleotide to the primer of the DNA substrate used. The n (non-extended) and $n+1$ (extended by one dNTP) DNA were resolved on a denaturing 20% polyacrylamide gel (Sequel NE, American Bioanalytical). To measure product formation as a function of time, the gels were scanned using a Storm 840 PhosphorImager (Amersham Biosciences) and quantified with the accompanying ImageQuant software. The data were analyzed using the Kaleidagraph program (Synergy software). Data from the burst experiments were fit to the burst equation: [product] = $A(1 - \exp(-k_{obs}t) + k_{SS}t)$. Data from active site titrations were fit to the quadratic equation: [E-DNA] = $0.5(K_{D(DNA)} + [E]_0 + [D]_0) - [0.25(K_{D(DNA)} + [E]_0 + [D]_0)^2 - ([E]_0[D]_0)]^{0.5}$, where [$E$-DNA] is the concentration of the Polβ-DNA complex, $[E]_0$ is the initial enzyme concentration, $[D]_0$ is the initial concentration of the gapped DNA substrate, and $K_{D(DNA)}$ is the dissociation constant of the Polβ-DNA complex. Single turnover kinetic data were fit to the single exponential equation: [product] = $A(1 - \exp(-k_{obs}t))$, where A is the amplitude, t is the time, and k_{obs} is the observed rate constant. Observed rate constants were then plotted against [dNTP], and the data were fit to the hyperbolic equation: $k_{obs} = k_{pol}[dNTP]/(K_d + [dNTP])$, where k_{pol} is the maximum rate of polymerization, and K_d is the equilibrium dissociation constant for dNTP. Fidelity values were calculated as follows: fidelity = $((k_{pol}/k_d)_c + (k_{pol}/k_d)_i)/((k_{pol}/k_d)_i)$, where c and i represent the correct and incorrect dNTPs, respectively.

RESULTS

I260Q Exhibits a Burst of Product Formation—The I260Q variant was previously isolated from a genetic screen of *in vivo* mutator mutants. The mutator tendencies of this variant were previously confirmed using the *in vitro* missing base primer extension assay (19). In the study described here, we use kinetic analyses to fully characterize this mutant and describe the kinetic basis for its mutator phenotype. First, we wished to determine whether the presteady-state kinetic profile of I260Q is similar to wild type. The reaction conditions are described under "Experimental Procedures." As shown in Fig. 1, I260Q displays biphasic kinetics of presteady-state nucleotide incorporation as does wild type, in which an initial rapid phase is followed by a slower, linear one. This is immediately followed by the rate-limiting step of the catalytic cycle, dissociation from DNA (25). For I260Q, the fast phase occurs at a rate of 11.4 ± 2.5 s^{-1}, which is similar to the 13.6 ± 1.3 s^{-1} for wild type on

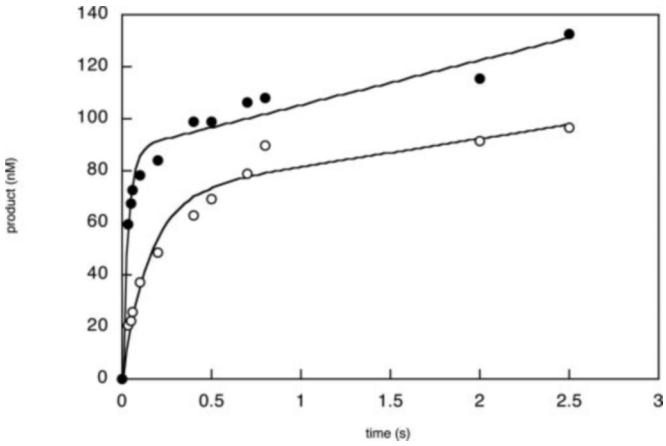

FIG. 1. **I260Q exhibits a burst of product formation.** Insertion of dTTP opposite template A was measured as a function of time using the KinTek apparatus at 37 °C. A solution of 100 nM I260Q or wild type preincubated with 300 nM DNA substrate was reacted with a solution of 100 μM dTTP containing 10 mM $MgCl_2$. The reactions were quenched with 0.5 M EDTA, and product formation was monitored as described under "Experimental Procedures." The DNA substrate employed in these experiments was 1B-A. The data for wild type (●) were fitted to the burst equation with a k_{obs} of 13.6 ± 1.3 s^{-1} and a steady state rate constant of 0.9 s^{-1}. The data for I260Q (○) were fitted to the burst equation with a k_{obs} of 11.4 ± 2.5 s^{-1} and a steady state rate constant of 0.4 s^{-1}.

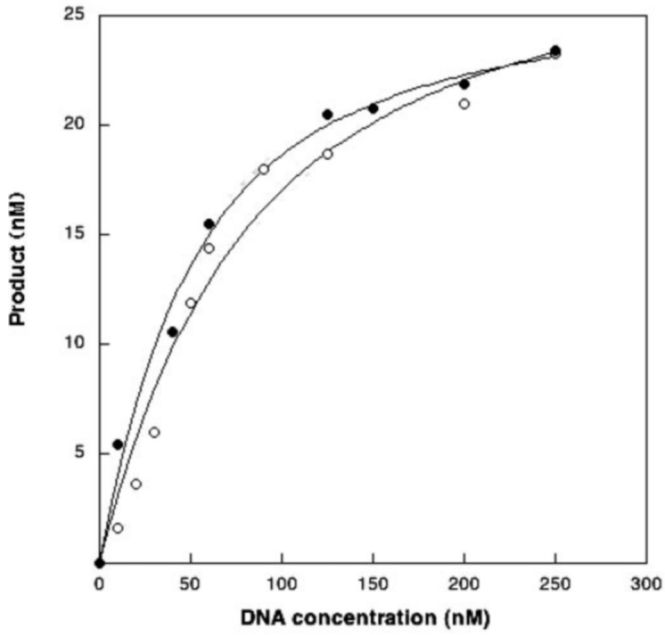

FIG. 2. **I260Q has a slightly higher affinity for the DNA substrate than wild type.** Insertion of dTTP opposite template A was monitored as a function of DNA substrate concentration. The enzyme was preincubated with various DNA concentrations ranging from 10 to 300 nM followed by mixing with a solution of 100 μM dTTP and 10 mM $MgCl_2$ for 0.3 s. The reactions were terminated, resolved, and analyzed as described under "Experimental Procedures." The *solid lines* represent the best fit to the quadratic equation. *A*, data for wild type were fit to the quadratic equation with a K_D of 60 nM. *B*, data for I260Q were fitted to the quadratic equation with a K_D of 35 nM.

this particular DNA substrate. The slower phase occurs at 0.4 s^{-1} and 0.9 s^{-1} for I260Q and wild type, respectively. The biphasic nature of the burst indicates that the I260Q variant, like wild type, has its rate-limiting step of the catalytic cycle after phosphodiester bond formation.

I260Q Has a Slightly Higher Affinity for the DNA Substrate than Wild Type—We used the active site titration assay to measure the dissociation constant of wild type or I260Q from the DNA substrate. Shown in Fig. 2 are the data obtained from these measurements fitted to the quadratic equation as described under "Experimental Procedures." From this experiment, the K_D values were calculated to be 35 nM for I260Q and 60 nM for wild type. Thus, the equilibrium dissociation constants are very similar for the two enzymes with I260Q having a slightly greater affinity for the DNA substrate.

I260Q Forms All Three dNTP Mispairs Opposite Both a Purine (A) and a Pyrimidine (C)—We wished to determine the kinetic basis for the mutator phenotype of I260Q previously observed in both *in vivo* and *in vitro* assays (19). First, we measured the rates and dissociation constants for the dNTP substrate for correct and incorrect nucleotide incorporation opposite template A in substrate 1B-A. The reaction conditions and molar ratios are listed under "Experimental Procedures." As illustrated in Fig. 3 for incorporation of the correct nucleotide, the results were first fitted to the single exponential equation for each individual dTTP concentration to calculate the k_{obs} for each of the dTTP concentrations used. These rates were then plotted as a function of dTTP concentration (Fig. 3*B*) and fitted to the hyperbolic equation to obtain the K_d and k_{pol} values. As summarized in Table II, the kinetic basis for the increased ability to misincorporate nucleotides opposite purine A is in the dissociation constant, K_d, for the dNTP. The dissociation constant for the correct dNTP substrate, dTTP in this case, is ~5-fold higher than wild type: 30 μM for I260Q and 6 μM for wild type, whereas the dissociation constant for the incorrect nucleotide is lower than wild type. For example, when dGTP is incorporated opposite A, the K_d for I260Q is 49 μM, whereas it is 147 μM for wild type. A similar difference between I260Q and wild type is observed for dATP misincorporation opposite A where I260Q has a K_d of 30 μM and wild type has a k_d of 138 μM. The K_d values for both wild type and mutant are lowered in reactions examining dCTP insertion opposite A most likely because of a slippage phenomenon that has previously been demonstrated for wild type. Because of slippage, the enzyme positions the base immediately 5′ to the template for nucleophilic attack thus allowing it to pair with the incoming nucleotide. In this case, this would mean incorporation opposite G rather than A, which could then form the Watson-Crick G-C base pair. The rate of incorporation for each dNTP substrate is similar for wild type and I260Q. This ultimately results in a lowered catalytic efficiency for I260Q for the correct dNTP substrate. However, I260Q has a somewhat higher catalytic efficiency than wild type for misincorporation. These data suggest that I260Q misincorporates nucleotides opposite purine A because of a lack of discrimination during substrate binding.

We also wished to examine misincorporation opposite a pyrimidine. We constructed a substrate with a templating C within the same sequence context as for A above. Table III summarizes the results of incorporation opposite pyrimidine C using template 1B-C. As observed with misincorporation opposite A, the I260Q variant also misincorporates opposite C. The kinetic basis for misincorporation opposite template C is K_d, the equilibrium dissociation constant. In fact, I260Q appears to prefer the incorrect dNTP substrate. The rates of correct and incorrect incorporation are comparable between wild type and I260Q as observed for insertion opposite template A. The catalytic efficiency of I260Q for misincorporation is slightly higher than that of wild type. This indicates that the basis for the misincorporation phenotype of I260Q and lowered fidelity observed in the *in vivo* and *in vitro* assays previously described results from decreased discrimination during dNTP binding by Polβ.

DISCUSSION

The I260Q Polβ variant was identified in a genetic screen as an enzyme with an overall activity similar to wild type Polβ but

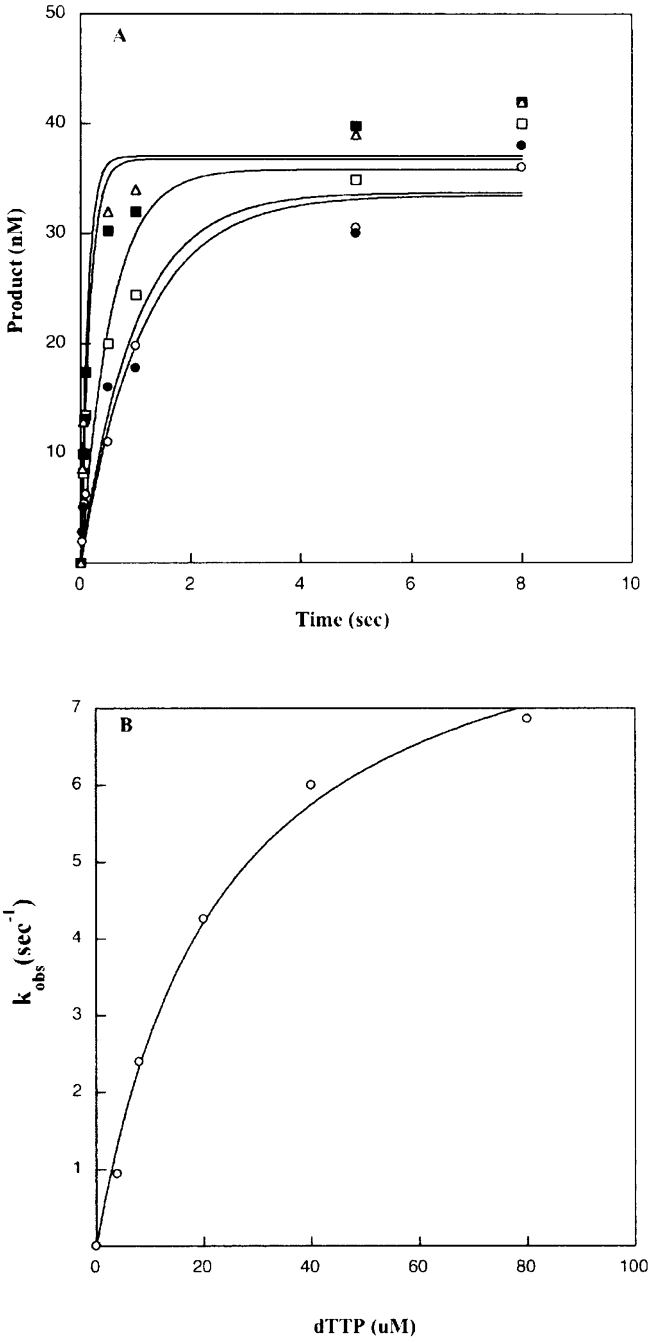

FIG. 3. **Single turnover experiments of correct nucleotide incorporation opposite adenine for I260Q.** *A*, incorporation of dTTP opposite A for I260Q at 37 °C. A preincubated solution containing 750 nM enzyme and 50 nM radiolabeled gapped DNA substrate was reacted with a solution of 10 mM $MgCl_2$ and 4 (○), 8 (●), 20 (□), 40 (■), or 80 (Δ) μM dTTP. The reactions were quenched, and product formation was monitored as described under "Experimental Procedures." The data were fitted to a single exponential equation to obtain k_{obs} for each dTTP concentration. *B*, secondary plot of k_{obs} (*y* axis) against dTTP concentration (*x* axis). The data were fitted to the hyperbolic equation as described under "Experimental Procedures"; the *solid line* represents the best fit of the data.

with a significantly lower fidelity (19). In this study, we describe the kinetic basis for the mutator phenotype of I260Q Polβ. Strikingly, I260Q binds the correct nucleotide with significantly lower affinity and incorrect nucleotides with 2–6-fold higher affinities than the wild type enzyme. Therefore, the kinetic basis for the mutator phenotype of I260Q lies in its inability to discriminate the correct from the incorrect dNTP during the binding step of nucleotide incorporation. Because residue 260 is located on the inside lining of the hydrophobic pocket within the hinge region that is between the catalytic and the COOH-terminal domains of Polβ, our kinetic data suggest that this hinge and the associated domain motions are important for polymerase fidelity.

The Hinge Functions in the Geometric Alignment of Substrates—The hinge region is located at the interface between the catalytic domain (residues 149–262) and the COOH-terminal domain (residues 263–338) of Polβ. Both domains present residues toward the large active site cleft that are crucial for template binding, nascent base pair recognition, and catalytic turnover (14–16). Strands β2, β7, and helix M are located close to the hinge axis, and the network of interactions extending from the residues in this region is likely to moderate the extent of domain motions. Careful analysis of the relative domain motions observed in various Polβ-substrate complexes identified the loops near Val-177 and Cys-178 and Pro-261, Lys-262, and Asp-263 as hinge boundaries. The flexibility of the two loops allows for the bulk movement of secondary structural elements within the COOH-terminal domain. Other residues, including but not limited to Leu-194, Thr-196, Cys-178, Ile-260, Gly-268, Val-269, and Phe-272, contribute interactions necessary for the maintenance and function of an intricate hydrophobic network along the hinge region. Some of these side chains also display obvious movements upon domain closure. Therefore, it is conceivable that the hinge, as orchestrated by the movement of some of these residues, controls the extent and the dynamics of the enzyme closure around the substrates (15, 16). Arg-258, Tyr-271, Arg-283, Asn-294, Glu-295, and Tyr-296 are layered immediately above the hydrophobic hinge region and form a major part of the template binding site. Rotation of the COOH-terminal domain results in enzyme activation by positioning the template, the 3′-OH of the primer, the base, and the α-phosphate of the incoming dNTP such that rapid and accurate nucleotide incorporation can occur.

Ile-260 Is Critically Involved in Domain Closure—Ile-260 is located near the hinge axis and in the wild type enzyme contributes to the formation of a hydrophobic core. Upon comparison of several high-resolution Polβ co-crystal structures, the Ile-260 side chain is consistently found in either of two different conformations. The χ2 angle changes such that Cδ is alternating between the "up" and the "down" position, thereby affecting the packing against the adjacent hydrophobic residues. Interestingly, the volume of a small cavity above Ile-260 appears to be altered by the χ2 switch as well. This cavity, as depicted in Fig. 4, could feasibly act as a buffer space absorbing local motions and allowing a specific flexing in the hinge between the COOH-terminal and the catalytic domains of Polβ.

The mutation from Ile-260 to Gln is associated with a slight change in side chain volume as well as a significant change in chemical nature. When altered from Ile to Gln, the small cavity above position 260 disappears. If the side chain amide group moves into the interior of the protein core, the hydrophobic packing would most likely be disrupted. However, analysis of the three most frequent rotamers using PYMOL along with molecular modeling indicate that the amide side chain is most likely oriented away from the adjacent hydrophobic residues and points toward the charged residues on the surface of the template binding cleft. These local changes could result in a polymerase that may not close properly and efficiently, thereby leading to a less stable but active conformation in the I260Q variant as compared with wild type Polβ. Aberrant positioning of the dNTP-binding residues within the active site of the enzyme could certainly affect dNTP affinity in the mutant

TABLE II
I260Q extends the primer with all three incorrect nucleotides opposite purine A

The correct pair is in bold.

Base pair	Enzyme	k_{pol}	K_d[a]	k_{polc}/k_{poli}[b]	K_{di}/K_{dc}[c]	k_{pol}/K_d	Fidelity[d]	WT[e]/Q
		s^{-1}	μM			$M^{-1}\ s^{-1}$		
A:dTTP	WT	10.2 ± 0.5	6 ± 1			1.70		
	I260Q	11.1 ± 1.2	30 ± 0.7			0.36		
A:dATP	WT	0.015 ± 0.0016	138 ± 42	680	23	0.00011	15,456	23
	I260Q	0.016 ± 0.0008	30 ± 4	694	1	0.00054	668	
A:dGTP	WT	0.013 ± 0.0003	147 ± 10	785	25	0.000088	19,319	19
	I260Q	0.017 ± 0	49 ± 0	647	1.6	0.000347	1,038	
A:dCTP	WT	0.010 ± 0.0005	20 ± 3	1030	3.3	0.00050	3,401	20
	I260Q	0.019 ± 0.004	9 ± 1	579	0.3	0.0021	172	

[a] Units are micromolar.
[b] The k_{pol} for correct (c) is divided by k_{pol} for incorrect (i).
[c] The K_d for incorrect (i) divided by the K_d for correct (c).
[d] Fidelity (F) is calculated as follows: $[(k_{pol}/K_d)c + (k_{pol}/K_d)i]/[(k_{pol}/K_d)i]$, where c and i represent correct and incorrect dNTPs respectively.
[e] WT, wild type.

TABLE III
I260Q efficiently forms all 3 dNTP mispairs opposite pyrimidine C

The correct pair is in bold.

Base pair	Enzyme	k_{pol}	K_d[a]	k_{polc}/k_{poli}[b]	K_{di}/K_{dc}[c]	k_{pol}/K_d	Fidelity[d]	WT[e]/Q
		s^{-1}	μM			$M^{-1}\ s^{-1}$		
C:dGTP	WT	11.5 ± 0.14	6 ± 1			1.91		
	I260Q	10.3 ± 0.57	42 ± 5			0.24		
C:dATP	WT	0.013 ± 0.0003	42 ± 4	885	7	0.00031	6,162	24
	I260Q	0.014 ± 0.001	15 ± 2	736	0.4	0.00093	259	
C:dTTP	WT	0.015 ± 0.00054	66 ± 8	767	11	0.00023	8,305	16
	I260Q	0.017 ± 0.00001	36 ± 0	606	0.9	0.00047	511	
C:dCTP	WT	0.0023 ± 0.0	15 ± 2	5,000	2.5	0.00015	12,734	30
	I260Q	0.0028 ± 0.0003	5 ± 1	3,679	0.1	0.00056	430	

[a] Units are micromolar.
[b] The k_{pol} for correct (c) is divided by k_{pol} for incorrect (i).
[c] The K_d for incorrect (i) divided by the K_d for correct (c).
[d] Fidelity (F) is calculated as follows: $[(k_{pol}/K_d)c + (k_{pol}/K_d)i]/[(k_{pol}/K_d)i]$, where c and i represent correct and incorrect dNTPs, respectively.
[e] WT, wild type.

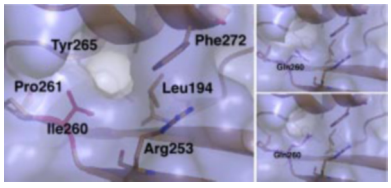

FIG. 4. **Molecular surface representation of polymerase β (Protein Data Bank code 9icx) highlighting structural features in the hinge region at the domain interface of palm and fingers.** *Left panel*, residue Ile-260 (*pink*) and neighboring template-binding residues (shown in atom color) are labeled. The empty space between Ile-260, Leu-194, and Phe-272 may serve to absorb relative domain motions along the hinge during the catalytic cycle of polymerase β. *Right panels*, residue Gln-260 (*red*) modeled with the two most frequently occurring rotamers (*top* and *bottom panels*, respectively). The mutation clearly decreases the volume of the cavity and, thus, hampers closure of the fingers domain around the incoming nucleotide and bound template DNA.

enzyme. This suggestion is consistent with the recently published structures of the wild type enzyme in complex with mismatched bases at the active site (26). They indicate that there might be an intermediate so-called "semi-open" complex that occurs after dNTP binding but before chemistry (26). The complexes showed that the bases stagger and form alternate hydrogen bonds with the surrounding polymerase residues. Such staggered bases partially overlap, thus preventing the fingers from properly closing and forming the optimal active site (26). We suggest that the active site of I260Q may also be in a semi-open conformation.

I260Q Is Important for dNTP Binding and Positioning—Molecular modeling suggests that the change of Ile-260 to Gln introduces small but significant shifts in adjacent hydrophobic residues that form part of the dNTP binding pocket, namely Tyr-271 and Phe-272 (15). Reordering of these side chains adjacent to the ribose moiety of the incoming dNTP affects nucleotide binding as has been shown by biochemical studies published previously (27). Alteration of Phe-272 to Leu leads to a decrease in the binding affinity for the dNTP substrate and an enzyme with lower fidelity (28). Asn-279, a direct spatial neighbor of Phe-272, forms a minor groove interaction with the incoming substrate such that incorrect dNTPs most likely protrude into the minor groove and clash with Asn-279. Alteration of Asn-279 to Ala results in an inaccurate enzyme with significantly less affinity for correct dNTP substrate (29). The reshaping of the dNTP binding pocket geometry when Ile-260 is altered to Gln is consistent with the finding that the I260Q Polβ shows a 5-fold increase in preference for the incorrect over the correct substrate during the binding step. Thus, we suggest that wild type Polβ does discriminate correct from incorrect substrates during dNTP binding and during subsequent steps in the catalytic cycle and not only during transition state chemistry, as has been proposed previously (30).

Ile-260 Is Important for Template Positioning—Based upon our modeling studies, changes in the size and the chemistry of residue 260 would be predicted to cause significant shifts in the position of surface residues of the COOH-terminal domain. As a result, the position of the template DNA could be critically affected, which in turn has long range effects on the geometry of the Watson-Crick binding pocket. The templating base forms an integral part of the Watson-Crick binding pocket and an aberrant geometry could be more permissive for accepting and incorporating the incorrect dNTP. This possibility has been explored and substantiated by molecular modeling studies. In

our modeling studies, we have found changes in the side chain positions of residues Arg-258, Glu-295, and Tyr-296 as a result of altering Ile-260 to Gln. Consequently, the template DNA is repositioned relative to where it would be expected to be found in the wild type enzyme, thereby affecting the position of the templating base and changing the geometry of the Watson-Crick binding pocket. The subtle structural changes described above could conceivably explain why the I260Q variant has a lower affinity for the correct dNTP substrate and higher affinity than the parent enzyme for the incorrect dNTP substrate, thus, leading to a significant drop in fidelity as compared with wild type Polβ.

Summary and Implications—Our data show that changing hinge residue 260 of Polβ from Ile to Gln results in a polymerase that has nearly wild type activity but is a mutator mutant. We find that the kinetic basis for misincorporation by I260Q lies in loss of discrimination at the level of dNTP substrate binding. Our modeling studies indicate that the Gln mutant affects the domain closure around the DNA substrate, that the protein matrix around the ribose moiety of the incoming nucleotide is altered, and that the DNA template could be positioned differently in this variant than in the wild type enzyme (19). DNA binding is the first step in the catalytic cycle, and it is likely that repositioning of the DNA substrate would consequently affect the subsequent steps, particularly dNTP binding and chemistry. Based on our finding that the I260Q variant has a decreased affinity for the correct nucleotide and increased affinity for the incorrect one, we propose that this mutant is less well adapted to form a nucleotide binding pocket with a geometry similar to that of wild type Polβ that supports catalysis. Subtle changes in a small and compact enzyme such as Polβ can have dramatic effects, making it an excellent model to further our understanding of mechanistic aspects of polymerase fidelity.

Acknowledgments—We thank members of the Sweasy laboratory for helpful discussions.

REFERENCES

1. Horton, J. K., Baker, A., Berg, B. J., Sobol, R. W., and Wilson, S. H. (2002) *DNA Repair* (*Amst.*) **1,** 317–333
2. Ochs, K., Sobol, R. W., Wilson, S. H., and Kaina, B. (1999) *Cancer Res.* **59,** 1544–1551
3. Dianov, G., Price, A., and Lindahl, T. (1992) *Mol. Cell. Biol.* **12,** 1605–1612
4. Barnes, D. E., and Lindahl, T. (2004) *Annu. Rev. Genet.* **38,** 445–476
5. McCullough, A. K., Dodson, M. L., and Lloyd, R. S. (1999) *Annu. Rev. Biochem.* **68,** 255–285
6. Raffoul, J. J., Cabelof, D. C., Nakamura, J., Meira, L. B., Friedberg, E. C., and Heydari, A. R. (2004) *J. Biol. Chem.* **279,** 18425–18433
7. Wilson, T. M., Rivkees, S. A., Deutsch, W. A., and Kelley, M. R. (1996) *Mutat. Res.* **362,** 237–248
8. Matsumoto, Y., and Kim, K. (1995) *Science* **269,** 699–702
9. Prasad, R., Singhal, R. K., Srivastava, D. K., Molina, J. T., Tomkinson, A. E., and Wilson, S. H. (1996) *J. Biol. Chem.* **271,** 16000–16007
10. Jonason, A. S., Baker, S. M., and Sweasy, J. B. (2001) *Chromosoma* (*Berl.*) **110,** 402–410
11. Plug, A. W., Clairmont, C. A., Sapi, E., Ashley, T., and Sweasy, J. B. (1997) *Proc. Natl. Acad. Sci. U. S. A.* **94,** 1327–1331
12. Gu, H., Marth, J. D., Orban, P. C., Mossmann, H., and Rajewsky, K. (1994) *Science* **265,** 103–106
13. Kunkel, T. A. (1985) *J. Biol. Chem.* **260,** 5787–5796
14. Sawaya, M. R., Pelletier, H., Kumar, A., Wilson, S. H., and Kraut, J. (1994) *Science* **264,** 1930–1935
15. Pelletier, H., Sawaya, M. R., Kumar, A., Wilson, S. H., and Kraut, J. (1994) *Science* **264,** 1891–1903
16. Pelletier, H., Sawaya, M. R., Wolfle, W., Wilson, S. H., and Kraut, J. (1996) *Biochemistry* **35,** 12742–12761
17. Arndt, J. W., Gong, W., Zhong, X., Showalter, A. K., Liu, J., Dunlap, C. A., Lin, Z., Paxson, C., Tsai, M. D., and Chan, M. K. (2001) *Biochemistry* **40,** 5368–5375
18. Starcevic, D., Dalal, S., and Sweasy, J. B. (2004) *Cell Cycle* **3,** e71–e74
19. Starcevic, D., Dalal, S., and Sweasy, J. B. (2004) *Biochemistry* **44,** 3775–3784
20. Sweasy, J. B., and Loeb, L. A. (1992) *J. Biol. Chem.* **267,** 1407–1410
21. Washington, S. L., Yoon, M. S., Chagovetz, A. M., Li, S. X., Clairmont, C. A., Preston, B. D., Eckert, K. A., and Sweasy, J. B. (1997) *Proc. Natl. Acad. Sci. U. S. A.* **94,** 1321–1326
22. Kosa, J. L., and Sweasy, J. B. (1999) *J. Biol. Chem.* **274,** 35866–35872
23. Shah, A. M., Maitra, M., and Sweasy, J. B. (2003) *Biochemistry* **42,** 10709–10717
24. Johnson, K. A. (1995) *Methods Enzymol.* **249,** 38–61
25. Werneburg, B. G., Ahn, J., Zhong, X., Hondal, R. J., Kraynov, V. S., and Tsai, M. D. (1996) *Biochemistry* **35,** 7041–7050
26. Krahn, J. M., Beard, W. A., and Wilson, S. H. (2004) *Structure* (*Camb.*) **12,** 1823–1832
27. Vande Berg, B. J., Beard, W. A., and Wilson, S. H. (2001) *J. Biol. Chem.* **276,** 3408–3416
28. Li, S. X., Vaccaro, J. A., and Sweasy, J. B. (1999) *Biochemistry* **38,** 4800–4808
29. Kraynov, V. S., Werneburg, B. G., Zhong, X., Lee, H., Ahn, J., and Tsai, M. D. (1997) *Biochem. J.* **323,** 103–111
30. Showalter, A. K., and Tsai, M. D. (2002) *Biochemistry* **41,** 10571–10576